Road Boundary Detection and Tracking Using Monochrome Camera Images

Sarah Strygulec†, Dennis Müller*, Mirko Meuter*, Christian Nunn*, Sharmila (Lali) Ghosh*, Christian Wöhler†

* Delphi Electronics & Safety
42119 Wuppertal, Germany
{dennis.mueller, mirko.meuter}@delphi.com
{christian.nunn, lali.ghosh}@delphi.com

† TU Dortmund University
Image Analysis Group
44227 Dortmund, Germany
sarah.strygulec@tu-dortmund.de
christian.woehler@tu-dortmund.de

***Abstract*—In this paper a method for Road Boundary Detection and Tracking on monochrome camera images is presented. Using this approach, it is possible to recognize road boundaries in areas without lane markings. To describe the shape of the boundary a clothoid road model is used. The parameters of this model are estimated and tracked by a Particle Filter. The implemented Particle Filter is based on the well known Condensation Algorithm. Only texture features are used for road recognition. For evaluation of these features a patch-based classifier is used. Based on a set of sequences the probability distribution of the classifier output is empirically determined. So the single patches can be assigned to "road" or "non-road" class with a certain probability. The presented algorithm shows good performance with reliable results on a variety of recorded video sequences.**

I. Introduction

The detection and tracking of road boundaries is an important task in driver assistance, since it highly improves the driver's safety by lane departure warning or even lane keeping. Many reliable systems for lane detection based on lane markings already exist. Most of these systems rely on Kalman Filters for estimation of the parameters of a road model, as e.g. the one proposed by Dickmanns and Zapp [1]. However, robust and reliable systems are required which are also capable of detecting road boundaries in regions with weak or especially no markings like rural roads. The method presented in this paper recognizes boundaries on roads without lane markings using only a single monochrome camera. The distinctiveness of the proposed approach among others is the utilization of a classifier for the measurement extraction within the Particle Filter framework.

During the past years the Particle Filter approach [2] [3] gained increasing relevance for tracking purposes, since it shows certain advantages compared to the Kalman Filter. The Particle Filter has a non-parametric representation and is therefore not restricted to Gaussian distributions. Hence, for example multimodal distributions can be tracked. The Particle Filter also provides the possibility to incorporate region based measurements like texture information. Southall [4] described a Particle Filter approach which is also restricted to lane markings. Often various image cues like edge, color or texture features are fused in Particle Filter based systems. For example Apostoloff and Zelinsky [5] extracted information on lane markings and fused them with edge and color features. In [6] an approach is given that recognizes road boundaries on roads without lane markings by fusing intensity, edge, color and texture features. In some systems the vanishing point is determined and used for initialization of a tracker [7] or a road segmentation [8]. It is obvious, that for a robust detection and tracking on roads without lane markings most of the systems rely on the evaluation of many different features. The presented approach shows promising results only using one kind of feature.

Visual tracking is highly relevant, since simple camera systems are quite inexpensive. Due to the fact that a camera image provides the possibility to acquire a huge amount of information for many different applications it is imaginable that in the future most vehicles will be equipped with a camera system. The detection and tracking based on monochrome camera images is a challenging task. Compared to other systems that provide additional color or depth information (stereo cameras), a smaller variety of potential cues is given. An example for the use of stereo vision is given in [9]. A system providing distance information is capable of detecting curbsides, which are usually harder to detect with two-dimensional features due to their similarity to the road surface. Nevertheless, on rural roads usually no significant difference in depth between road and roadside is given, since the transition is often smooth. Using color or stereo cameras provide more information in special cases, but also increase the costs distinctly.

II. Recursive State Estimation

This section will give a brief introduction on the Particle Filter approach [2] [3] and a short overview of the implemented system. The distribution of the state x_k at time step k is represented by its density function $p(x_k|z_{0:k})$. This function is called posteriori density function and describes the probability of the state x_k to be the true state depending on the observations $z_{0:k}$ up to time step k. Assuming that the states originate from a markov process with temporal independent observations z_k the recursive Bayes equation [10] is obtained:

$$\begin{aligned} p(x_k|z_{0:k}) &= c_k \; p(z_k|x_k)p(x_k|z_{0:k-1}) \\ p(x_k|z_{0:k-1}) &= \int p(x_k|x_{k-1})p(x_{k-1}|z_{0:k-1})dx_{k-1} \end{aligned} \tag{1}$$

The probability $p(x_k|z_{0:k-1})$ is called the prior density function and represents the prediction of the actual density function based on the former posterior density $p(x_{k-1}|z_{0:k-1})$ at time step $k-1$. The probability for the transition from x_{k-1} to x_k is given by $p(x_k|x_{k-1})$. The prior density is multiplied by the likelihood function $p(z_k|x_k)$, which describes the probability to measure z_k under the hypothesis x_k. The multiplication with the likelihood function is also called observation update. To ensure that the integral of $p(x_k|z_{0:k})$ yields 1, the density is multiplied by the normalization constant c_k.

The Particle Filter allows a non-parametric representation of the posteriori density. The density is approximated by discrete samples (particles) x_k^i that are weighted by the factor w_k^i:

$$p(x_k|z_{0:k}) \approx \sum_i w_k^i \delta(x_k - x_k^i) \tag{2}$$

Because the posteriori density in time step k is not known before, the particles are sampled from a proposed importance density $q(x_k^i|x_{k-1}^i, z_k)$.

$$x_k^i \sim \; q(x_k^i|x_{k-1}^i, z_k) \tag{3}$$

Hence the weights w_k^i are given by

$$w_k^i \propto \frac{p(z_k|x_k^i)p(x_k^i|x_{k-1}^i)}{q(x_k^i|x_{k-1}^i, z_k)} w_{k-1}^i \tag{4}$$

under the constraint

$$\sum_i w_k^i = 1 \tag{5}$$

A convenient way to choose the importance density is

$$q(x_k^i|x_{k-1}^i, z_k) = p(x_k^i|x_{k-1}^i) \tag{6}$$

which then yields the following under the constraint (5)

$$w_k^i \propto p(z_k|x_k^i) w_{k-1}^i \tag{7}$$

In this case only the likelihood needs to be determined to update the weights.

For the presented application the implementation of the Particle Filter is based on the CONDENSATION algorithm proposed by Isard and Blake [2]. With the Particle Filter the parameters of a potential road boundary are estimated. The model which is used for representation of a road boundary and the resulting state vector are described in Section III. An overview of the corresponding system is given by Figure 1. The dynamic system in state space is described by the evolution function (8) and the measurement function (9), with v_k denoting the process noise and n_k denoting the measurement noise.

$$x_k = f_k(x_{k-1}, v_k) \tag{8}$$

$$z_k = h_k(x_k, n_k) \tag{9}$$

As explained before the Particle Filter basically performs two steps: the prediction and the observation update. The transition from x_{k-1} to x_k is realized by a dynamic model which describes the evolution process (8). The dynamic model is also explained in more detail in Section III. The prediction of x_k is followed by the observation process. As an input to the observation process a monochrome camera image is available. The measurements z_k are extracted from this image. The determination of the measurements is described by the

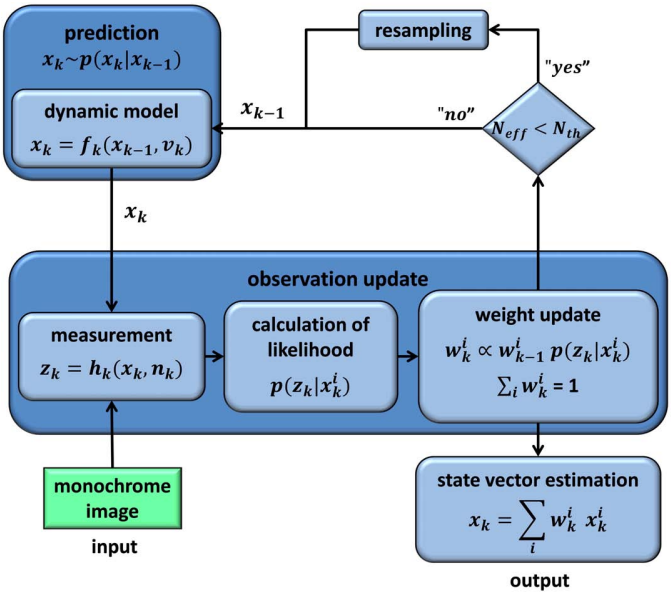

Fig. 1. Overview of the used Particle Filter system showing the main steps of state vector estimation

observation function in (9). In the presented algorithm the measurements z_k are provided by a texture classifier. More information on the classifier and its features is given in Section IV. Based on these measurements the observation likelihood $p(z_k|x_k^i)$ for each sample i is calculated. This procedure is explained in Section V. Afterwards it is possible to recursively calculate the new weights w_k^i based on the prior weights w_{k-1}^i and the observation likelihood. Due to the way the likelihood is defined numerical problems arise, which highly influence the calculation of the weights. Section VI shows a way to solve this problem. Finally the distribution of the weighted particles can be evaluated to get an estimation for the true state x_k. Here the weighted sum of the samples is computed:

$$x_k = \sum_i w_k^i x_k^i \tag{10}$$

Based on the new posterior density function $p(x_k|z_{0:k})$ a resampling can be performed to increase the density of samples in regions with a high probability. In order to decide whether a resampling is beneficial the effective sample size N_{eff} is determined and compared to a threshold value N_{th}. N_{eff} can be estimated by

$$\hat{N}_{\text{eff}} = \frac{1}{\sum_i (w_k^i)^2} \tag{11}$$

After the resampling step the weights are uniformly distributed. For further information on resampling refer to [3].

III. Dynamic Model

For a representation of the road boundary in parameter space a three-dimensional road model is used. The commonly used clothoid road model [11] [12] has been chosen, due to its high relevance and flexibility in road analysis.

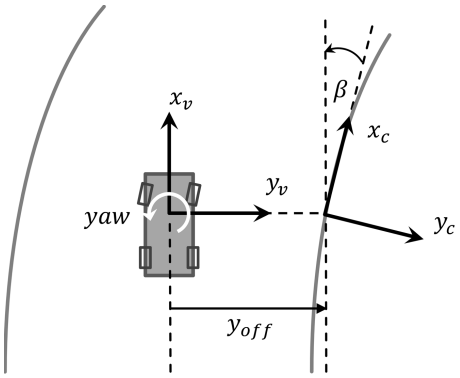

Fig. 2. Planar coordinate system showing the relation between the vehicle coordinate system (x_v, y_v) and the curvature coordinate system (x_c, y_c). The translation is given by the lateral offset y_{off} and the rotation is given by the heading angle β

$$\begin{aligned} x_{\text{v,rb}}(l) &= l \\ y_{\text{v,rb}}(l) &= \frac{1}{6}c_1 l^3 + \frac{1}{2}c_0 l^2 + \beta l + y_{\text{off}} \\ z_{\text{v,rb}}(l) &= 0 \end{aligned} \tag{12}$$

Here $x_{\text{v,rb}}$ denotes the longitudinal axis while $y_{\text{v,rb}}$ denotes the lateral and $z_{\text{v,rb}}$ the vertical axis. $(x_{\text{v,rb}}, y_{\text{v,rb}}, z_{\text{v,rb}})$ descirbes the position of the road boundary in the vehicle coordinate system. Only small angles are assumed, hence the longitudinal distance is approximately equal to the arc length l. Since only planar roads are considered, the vertical distance is set to 0. The parameters defining the lateral position are the lateral offset y_{off}, the heading angle β, the curvature c_0 and the curvature change rate c_1. Figure 2 illustrates relation between the vehicle coordinate system (x_v, y_v) and the curvature coordinate system (x_c, y_c). According to the parameters in (12), the following state vector results

$$X = \begin{pmatrix} y_{\text{off}} \\ \beta \\ c_0 \\ c_1 \end{pmatrix} \tag{13}$$

No other parameters were added to keep the number of parameters and thus the dimension of the filter small. Assuming no acceleration and constant yaw rate $\dot{\beta}$ during the time step dt the following dynamic model is achieved. The yaw rate and the velocity are inputs from internal sensors.

$$x_k = \begin{pmatrix} 1 & vdt & \frac{1}{2}(vdt)^2 & \frac{1}{6}(vdt)^3 \\ 0 & 1 & vdt & \frac{1}{2}(vdt)^2 \\ 0 & 0 & 1 & vdt \\ 0 & 0 & 0 & 1 \end{pmatrix} x_{k-1} + \begin{pmatrix} 0 \\ -dt \\ 0 \\ 0 \end{pmatrix} \dot{\beta} \tag{14}$$

IV. Measurement Extraction

The measurements z_k are the result of a neural network classifier, performing a texture classification on an image ROI. This ROI extends over the whole image width and possibly up to the horizon. At the current state the height of the ROI is fixed and the possibility of an incorporation of a horizon detection is investigated. For the purpose of feature extraction the image ROI is vertically and horizontally subdivided into uniform patches and several image-features are extracted on these regions. Figure 3 shows an example for the subdivided ROI. Each patch is classified based on these features and

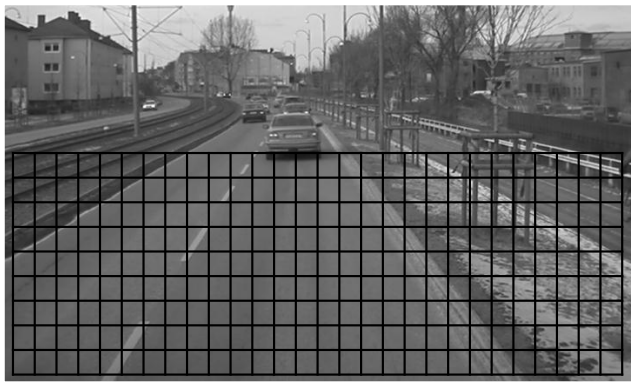

Fig. 3. ROI that is used for classification subdivided into equally sized image patches

assigned to "road" or "non-road" class. The classifier output spans an interval from $d_{\min}$ to $d_{\max}$. All values closer to $d_{\min}$ are assigned to "road" class and all values closer to $d_{\max}$ are assigned to "non-road" class.

To achieve more precise measurements a high resolution of patches would be beneficial. But with an increasing number of patches the computational effort increases and the patches need to have at least a certain size to provide accurate results. Despite that fact, one possibility to gain a higher horizontal resolution is a horizontal overlapping of the patches. For a good utilization the patches overlap by the half of their width. Applying this the number of horizontal patches raises from N_h to $2N_h - 1$ while the patch size remains equal. For efficient realization, the texture features are calculated on regions of half of the width of a patch. Afterwards the features of two neighboring regions are combined into one patch and passed to the classifier. Thus the features for the overlapping patches do not need to be recalculated and the computational effort is similar to the calculations without overlapping. Figure 4 illustrates the overlapping method. On the one hand this approach yields a higher effective horizontal resolution at a slight increase of computational costs. On the other hand the overlapping causes a correlation between the single patches. However, in the subsequent processing the effect of the correlation is assumed to be small so that the induced error can be neglected.

For training of the neural network a training set of 120 sequences with an average length of 30 seconds was manually annotated. 15 seconds per sequence have been used for the training process. The training set includes rural scenes as well as urban and freeway scenes. The trained classifier was tested on a set of 80 sequences, also including rural, urban and freeway scenes. The histograms in Figure 5 show the performance of the classifier on the test set. The white histogram shows the relative frequency for the data corresponding to the ground truth of the "road" class and the gray histogram

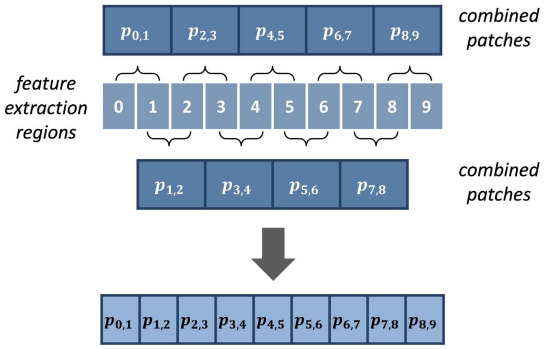

Fig. 4. Overlapping of patches: the patches for classification are combined from two neighboring feature extraction regions. E.g. patch $p_{0,1}$ is given by the combination of the features from region 0 and 1 whereas patch $p_{1,2}$ results from the features of region 1 and 2. Both patches are overlapping in region 1

corresponding to the ground truth of the "non-road" class. For evaluation the output interval $[d_{\min}, d_{\max}]$ is subdivided into 25 uniform bins $[d_0, d_1, ..., d_{24}]$. The relative number of misclassifications for values close to $d_{\min}$ or close to $d_{\max}$ is very small. So for values close to the bounds of the given interval the assignment is unambiguous. For values not close to the bounds the ratio is less unambiguous, but the absolute number of outputs in this regions is quite small. The classification results for each patch form the measurement vector $z_k \in [d_0, d_1, ..., d_{24}]$. The classifier outputs directly relate to a certain probability. According to the "confidence mapping" approach by Schürmann [13] the values can be mapped to a probability based on the histogram of frequencies. Equation (15) expresses the calculation of the probability for the "non-road" class for each bin d_i.

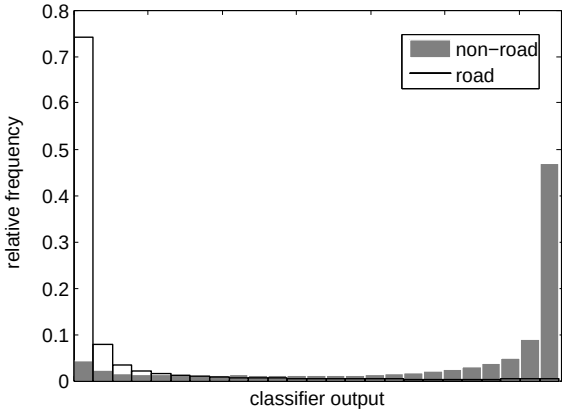

Fig. 5. Relative frequency of classifier output assigned to ground truth data (white and gray histogram) subdivided into 25 bins

$$conf_{\text{non-road}}(d_i) = \frac{hist(d_i|non\text{-}road)}{hist(d_i|non\text{-}road) + hist(d_i|road)} \tag{15}$$

The result of the confidence mapping is shown in Figure 6. The histograms in Figure 5 represent the empirically determined probability distribution of both classes, respectively. Assuming

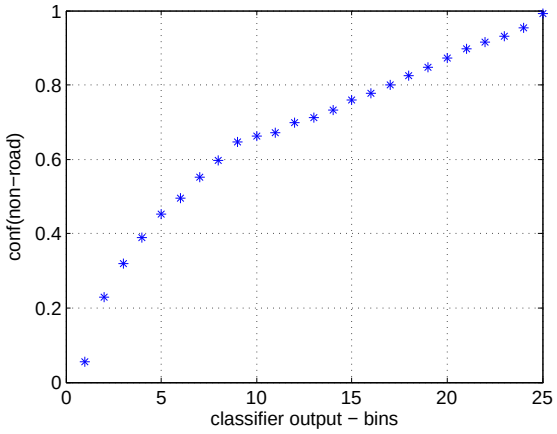

Fig. 6. Result of confidence mapping according to Eq.(15) [13] based on the classifier output which is shown in Figure 5

"road" or "non-road" the conditional probability for the outputs d_i can be approximated by

$$\begin{aligned} p(d_i|road) &\approx hist_{\text{road}}(d_i) \\ p(d_i|non\text{-}road) &\approx hist_{\text{non-road}}(d_i) \end{aligned} \tag{16}$$

V. Likelihood Calculation

To determine the likelihood $p(z_k|x_k^i)$ of a hypothesis x_k^i, which defines the shape and position of the road boundary, a projection of the corresponding three dimensional road model into the image plane is performed. For each vertical center of a patch row the corresponding longitudinal distance is known. Based on these distance values the corresponding points of the road model are projected. Hence for each patch row the horizontal position of the projected road model is calculated. The respective patch for each position is determined. Figure 7 illustrates this assignment on an image detail from figure 3. The grid represents the subdivision into patches. Let the white line be the projection of a road model, then the white dashes are the horizontal positions of the road model at the vertical centers of each patch row. The white squares denote the assigned patches. This procedure yields the corresponding patch index $idx_m(x_k^i)$ for every row m as a function of the hypothesis x_k^i.

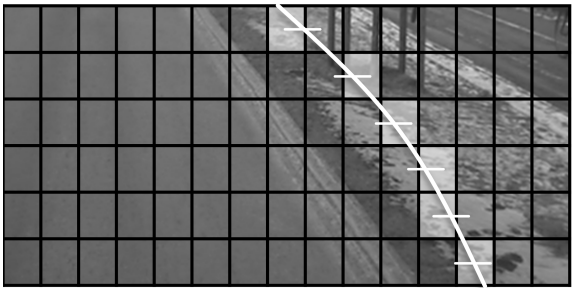

Fig. 7. Image detail from ROI for classification: Projection of the road model into the image plane, marked by the white line. The grid represents the subdivision into patches. A white dash marks the position of the projected road model at the vertical center of each patch row. The respective patches for the resulting positions at the vertical centers are marked in white color

Since the patch rows are statistically independent from each other, the likelihood $p(z_k|x_k^i)$ is given by the product of the

Fig. 8. Image detail from ROI for classification: Hypothesis for a right road boundary: The projection of the road model yields that the green patches to the left of the patch at position idx_m are supposed to be of "road" type and the red patches to the right of the patch at position idx_m are supposed to be of "non-road" type

likelihood for each row $p(z_{k,m}|x_k^i)$ over the number of rows N_r. $z_{k,m}$ denotes the measurements for row m at time step k:

$$p(z_k|x_k^i) = \prod_{m=0}^{N_r} p(z_{k,m}|x_k^i) \tag{17}$$

For calculation of $p(z_{k,m}|x_k^i)$ it is assumed that the patches of each row are also independent in horizontal direction, even though they are not in the strict sense (compare Section IV). The prior indexed patch $idx_m(x_k^i)$ at row m marks the position of the boundary and l denotes the horizontal position of a patch in row m. Patches in a certain neighborhood to this boundary should be of "road" type on one side and of "non-road" type on the other side. Figure 8 shows an example for the assumption of a right road boundary with up to five neighboring patches respectively. Here the green patches denote the ones supposed to be of "road" type and the red patches denote the ones supposed to be of "non-road" type. This interpretation of the hypothesis yields the following equations for a right boundary, taking into account N_l neighboring patches to the left and N_r neighboring patches to the right:

$$p(z_{k,m}|x_k^i) = \prod_l p(z_{k,m,l}|u(x_k^i)) \tag{18}$$

$$u(x_k^i) = \begin{cases} road & \text{if } l < idx_m(x_k^i) \\ non\text{-}road & \text{if } l > idx_m(x_k^i) \end{cases} \tag{19}$$

$$\begin{aligned} p(z_{k,m}|x_k^i) = & \prod_{l=idx_m(x_k^i)-N_l}^{idx_m(x_k^i)-1} p(z_{k,m,l}|road) \\ & * \prod_{l=idx_m(x_k^i)+1}^{idx_m(x_k^i)+N_r} p(z_{k,m,l}|non\text{-}road) \end{aligned} \tag{20}$$

The first product in (20) corresponds to the green patches of one row in Figure 8 and the second product corresponds to the red patches. $z_{k,m,l}$ denotes the measurement at patch position (m, l). Since $z_k \in [d_1, d_2, ..., d_{24}]$ the probability distributions $p(z_{k,m,l}|road)$ and $p(z_{k,m,l}|non\text{-}road)$ are given by

$$\begin{aligned} p(z_{k,m,l}|road) &= p(d_i|road) \\ p(z_{k,m,l}|non\text{-}road) &= p(d_i|non\text{-}road) \end{aligned} \tag{21}$$

These distributions are represented by the histograms in Section IV. The number of neighbors can of course be varied and be made independent from the left or the right side of the boundary. As an example the number of neighboring patches supposed to be of "road" type could be adapted to the lane width, such that as many patches as possible are taken into account. Since actually no reliable information on the lane width is given, the number of neighboring patches is restricted to a fixed number of five patches, respectively.

VI. Practical computation of weights

In practice the huge number of products during the calculation of the likelihood leads to numerical problems. Because of numerous multiplications of possibly very small probabilities the likelihood may results in an infinitesimal value. This can lead to a cancellation of the decimal places which are important to distinguish between the weightings. Without samples with a dominant weight no detection and thus no tracking is possible. To circumvent this problem it is a common approach to perform the computation of these products in the logarithmic domain. The products are thus replaced by the sum of the logarithmic likelihoods:

$$\begin{aligned} log(p(z_{k,m}|x_k^i)) = & \sum_{l=idx_m(x_k^i)-N_l}^{idx_m(x_k^i)-1} log(p(z_{k,m,l}|road)) \\ & + \sum_{l=idx_m(x_k^i)+1}^{idx_m(x_k^i)+N_r} log(p(z_{k,m,l}|non\text{-}road)) \end{aligned} \tag{22}$$

Under this condition the updated unnormalized weights are calculated as follows:

$$log(w_k^i) = log(w_{k-1}^i) + log(p(z_k|x_k^i)) \tag{23}$$

It is not appropriate to calculate the normalization of w_k^i in logarithmic scale, since this leads to the same numerical problem as mentioned above. But for numerically more stable calculations it is advantageous to normalize the logarithmic weights to their maximum. Afterwards the weights can be exponentiated and normalized to the sum of one.

$$\begin{aligned} log(\tilde{w}_k^i) &= log(w_{k-1}^i) - log(w_{k-1}^{max}) \\ log(w_{k-1}^{max}) &= max(log(w_{k-1}^i)) \end{aligned} \tag{24}$$

VII. Evaluation and Results

The presented method shows reliable results in different scenarios, for example urban or rural landscapes. The method has been tested in various situations like different weather conditions (sun, rain, snow) and different lighting conditions (cloudy, low angle of sun). For the test sequences the Particle

Filter used 200 particles and converged within only a few frames. Actually only one resulting parameter set is determined and the left and right boundary are estimated independently from each other. Figure 10 at the end of this paper shows some results for either a left or a right road boundary. The green line in Figure 10 marks the road boundary estimate and is given by the weighted sum of the whole particle set.

For evaluation the lateral offset of the road boundary has been manually labeled at close range for each frame. An area instead of a single line is used for labeling, since often no clear road boundary exists, especially on rural roads, and the geometry of the road boundary can not be fitted exactly. A parabolic model including the curvature and heading angle is used to project a curved area into the image plane. This area is shown in Figure 9 bounded by the white lines. The projected area can be vertically shifted to match the road boundary and determine the lateral offset which is given by the center of the labeled area (dashed line in Figure 9). Due to the propagation given by the dynamic model (Section III) the heading angle, curvature and the curvature change rate have a certain influence on the lateral offset, so that these parameters are also taken into account by evaluating the lateral offset.

The labeled area has a width of $30cm$ in world coordinates

Fig. 9. Labeled road boundary: The white lines mark the bounds of the labeled area. Each hypothesis within this area is assumed to match the road boundary. The dashed line marks the center of the area, which represents the ground truth of the lateral offset

to the left and to the right of the true boundary, respectively. For evaluation of the estimated road boundary it is determined whether the estimate is located within the labeled area or not. Additionally the root mean square error (RMSE) among the estimate and the labeled lateral offset is calculated. For that purpose the lateral offset of the estimated road boundary $\hat{y}_{\text{off}}$ is calculated for certain longitudinal distances d_x. Based on these values the match-rate at time step k is calculated:

$$match\text{-}rate_k = \frac{1}{N_x}\sum_{d_x}^{N_x} match(d_x) \tag{25}$$

$$match(d_x) = \begin{cases} 1 & y_{\text{label,l}}(d_x) < \hat{y}_{\text{off}}(d_x) < y_{\text{label,r}}(d_x) \\ 0 & \text{otherwise} \end{cases} \tag{26}$$

N_x denotes the number of lateral positions, $y_{\text{label,l}}$ denotes the left bound and $y_{\text{label,r}}$ the right bound of the labeled area. The average match-rate for a set of real sequences including about 5000 frames of labeled data is shown in table I. The RMSE for time step k is given by (27) with $y_{\text{label,c}}$ denoting the center of the labeled region:

$$RMSE_k = \sqrt{\frac{1}{N_x}\sum_{d_x}^{N_x}(y_{\text{label,c}}(d_x) - \hat{y}_{\text{off}}(d_x))^2} \tag{27}$$

The average RMSE (in meters) for all sequences is also shown in table I.

TABLE I. EVALUATION RESULTS

mean match-rate	0.7729
mean RMSE (m)	0.2957

The evaluation shows promising results. Problems arise when the surface of a sidewalk is very similar to that of the road and no significant difference during the transition to a sidewalk, for example no curbside, is given. Also heavily damaged or very dirty roads cause problems, since their surfaces appear to be highly textured similar to textures at road boundaries.

VIII. SUMMARY AND FUTURE WORK

In this paper a method for road boundary detection and tracking on monochrome camera images with a Particle Filter has been presented. Road boundaries can be reliably detected and tracked, even in areas without any kind of lane marking. A clothoid road model represents the road boundary and its parameters are estimated by the Particle Filter. The dimension of the Particle Filter is kept low by limiting the state vector to a minimum set of parameters. Information on the potential road boundary position in the monochrome image is obtained by a texture classifier. For classification a neural network has been trained which provides stable results. An efficient implementation for feature extraction, which makes use of overlapping regions, has been developed. To increase numerical stability and avoid the extinction of decimal places the calculation of the observation likelihood had been transformed to the logarithmic domain.

The left and right boundary are estimated independently of each other. Tracking both sides simultaneously, under the assumption of parallel lines, would increase the robustness of the estimation and provide additional information on the lane width. Based on the estimation for the lane width the number of neighboring patches for the likelihood calculation could be well defined. For this purpose, the dimension of the state vector will have to be extended by only one parameter.
The state is estimated by computation of the weighted sum of all samples. Nevertheless one advantage of the Particle Filter is the possibility to track multimodal distributions. Often, especially at forking or joining parts of the road, more than one hypothesis is available. Replacing the weighted sum by a clustering process would provide estimations for multiple hypothesis, since for example at a forking an new hypothesis is already tracked while the prior one is still present and a smooth transition would be possible.

ACKNOWLEDGMENT

This work was also supported by the European Commission under interactIVe, a large scale integrated project part of the FP7-ICT for Safety and Energy Efficiency in Mobility.
The authors would like to thank all partners within interactIVe for their cooperation and valuable contribution.

Fig. 10. Results of road boundary detection showing either the left or the right road boundary as a green line

REFERENCES

[1] E.D. Dickmanns and A. Zapp. A curvature-based scheme for improving road vehicle guidance by computer vision. In *Mobile Robots, SPIE Proc. Vol. 727, Cambridge, Mass.*, pages 161–168, 1986.

[2] M. Isard and A. Blake. Condensation - conditional density propagation for visual tracking. *International Journal of Computer Vision*, 29(1):5–28, 1998.

[3] N. Gordon J.S. Arulampalam, S. Maskell and T.Clapp. A tutorial on particle filters for online nonlinear/non-gaussian bayesian tracking. *Signal Processing, IEEE Transactions on*, 50(2):174 –188, feb 2002.

[4] B. Southall and C.J. Taylor. Stochastic road shape estimation. In *Computer Vision, 2001. ICCV 2001. Proceedings. Eighth IEEE International Conference on Computer Vision ICCV 2001*, volume 1, pages 205 –212 vol.1, 2001.

[5] N. Apostoloff and A. Zelinsky. Robust vision based lane tracking using multiple cues and particle filtering. In *Intelligent Vehicles Symposium, 2003. Proceedings. IEEE*, pages 558 – 563, june 2003.

[6] C. Knöppel U. Franke, H. Loose. Lane recognition on country roads. In *Intelligent Vehicles Symposium, 2007 IEEE*, pages 99 –104, june 2007.

[7] Yan Wang, Li Bai, and M. Fairhurst. Robust road modeling and tracking using condensation. *Intelligent Transportation Systems, IEEE Transactions on*, 9(4):570 –579, dec. 2008.

[8] Hui Kong, J.-Y. Audibert, and J. Ponce. General road detection from a single image. *Image Processing, IEEE Transactions on*, 19(8):2211 –2220, aug. 2010.

[9] U. Franke J.Siegemund and W.Forstner. A temporal filter approach for detection and reconstruction of curbs and road surfaces based on conditional random fields. In *Intelligent Vehicles Symposium (IV), 2011 IEEE*, pages 637 –642, june 2011.

[10] D.Fox S.Thrun, W.Burgard. *Probabilistic Robotics (Intelligent robotics and autonomous agents)*. MIT Press, 2006.

[11] E.D. Dickmanns and B.D. Mysliwetz. Recursive 3-d road and relative ego-state recognition. *Pattern Analysis and Machine Intelligence, IEEE Transactions on Pattern Analysis and Machine Intelligence*, 14(2):199 –213, feb 1992.

[12] A. Eidehall and F. Gustafsson. Combined road prediction and target tracking in collision avoidance. In *Intelligent Vehicles Symposium, 2004 IEEE*, pages 619 – 624, june 2004.

[13] Jürgen Schürmann. *Pattern classification - a unified view of statistical and neural approaches*. Wiley, 1996.